

### 3. CHARACTERISTICS

#### 3.1 Cathode voltage and current

The cathode voltage and current were measured by a high-voltage divider and a resistor, respectively, and the tube voltage was  $-1$  times the cathode voltage. Figure 4 shows variations in the voltage and current. The negative peak voltage increased when the input voltage from an auto transformer was increased. Next, the peak tube current was regulated constantly by the filament voltage.

#### 3.2 X-ray source

In order to measure images of the x-ray source, we employed a pinhole camera with a hole diameter of  $50 \mu\text{m}$  in conjunction with a Computed Radiography (CR) system.<sup>19</sup> The dimensions of small and large spots seldom varied and had values of approximately  $1 \times 1$  and  $4 \times 4 \text{mm}$ , respectively.

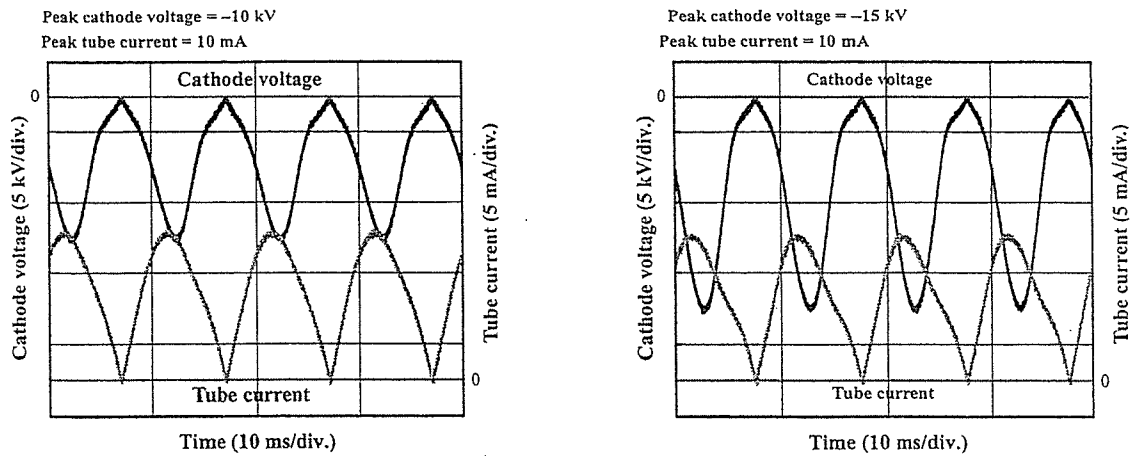


Fig. 4. Cathode voltages and tube currents at indicated conditions.

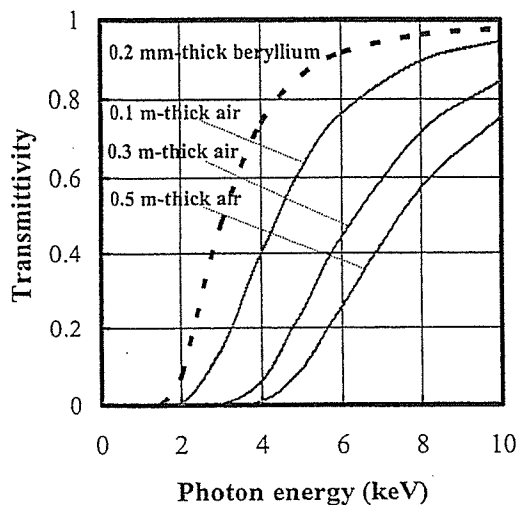


Fig. 5. Transmittivity of x rays with photon energy.

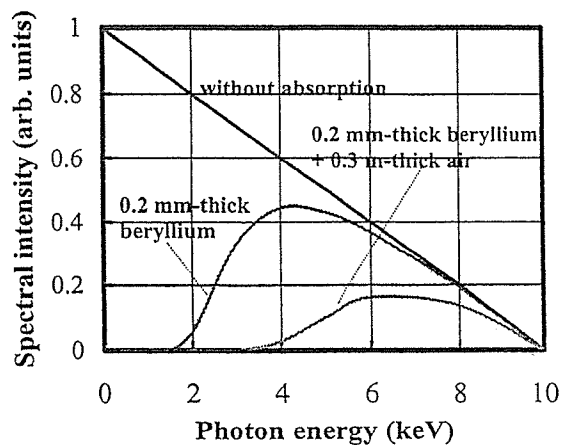


Fig. 6. Calculated bremsstrahlung spectra at indicated conditions.

### 3.3 X-ray spectra

Figure 5 shows transmittivity of beryllium and dry air with changes in the photon energy. When a 0.2 mm-thick beryllium window is employed, x-ray spectra with energies of lower than 2 keV are absorbed effectively. Subsequently, 0.5 m-thick air transmit x rays with energies of higher than 4 keV.

The bremsstrahlung x-ray spectra were calculated by the mass attenuation coefficients of the beryllium and the dry air at a constant tube voltage of 10 kV (Fig. 6). As shown in this figure, the soft x rays of lower than 2 keV were primarily absorbed by the beryllium x-ray window, and the rays were also absorbed by the air. Therefore, the distance should be decreased as much as possible in order to obtain soft x rays.

## 4. RADIOGRAPHY

The radiography was performed using the CR system (Konica Regius 150) and the small spot, and the distance between the x-ray source and imaging plate was 0.5 m. Next, the peak current ( $I_p$ ) and the exposure time were 10 mA and 10 s, respectively. Figure 7 shows radiograms of tungsten wires coiled around pipes made of polymethyl methacrylate with a peak tube voltage  $V_p$  of 15 kV. Although the image contrast increased with increases in the wire diameter, a 50  $\mu\text{m}$ -diameter wire could be observed.

A radiogram of a thin film for food wrapping is shown in Fig. 8. The  $V_p$  was 15 kV, and the image of a folded film is visible. Next, angiograms of rabbit hearts recorded using iodine microspheres of 15  $\mu\text{m}$  in diameter are shown in Fig. 9. These two images were obtained using a 1.0 mm-thick aluminum filter and without using the filter at a  $V_p$  of 15 kV. In the case where the filter was not employed, the coronary arteries were barely visible, since the heart did not transmit extremely soft x rays. Finally, Fig. 10 shows an angiogram of the external ear of a rabbit; iodine-based microspheres of 15  $\mu\text{m}$  in diameter were used at a  $V_p$  of 10 kV, and fine blood vessels of about 50  $\mu\text{m}$  were clearly visible.

## 5. DISINFECTION

Figure 11 shows the experimental setup for disinfection using soft x rays. Fungi were enclosed in an envelope and were exposed to soft x rays using the large spot, and we performed disinfection of three fungi with changes in the exposure time using a copper box with a  $V_p$  of 15 kV and an  $I_p$  of 10 mA. In these experiments, the complete disinfection times for *Bacillus subtilis* and staphylococcus were approximately 15 and 3 hours, respectively, and the time for *B-coli* was less than 1 hour (Tables 1-3).

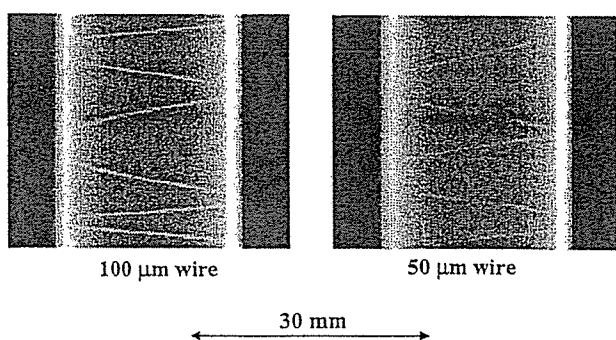


Fig. 7. Radiograms of tungsten wires of 50 and 100  $\mu\text{m}$  in diameter coiled around pipes made of polymethyl methacrylate.

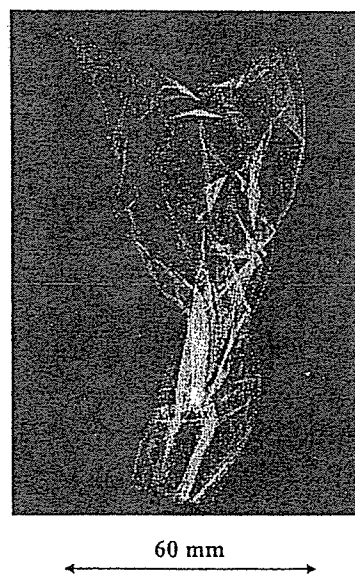


Fig. 8. Radiogram of film.

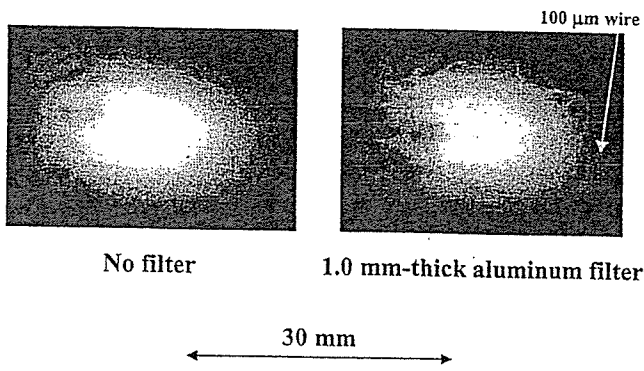


Fig. 9. Angiograms of rabbit hearts.

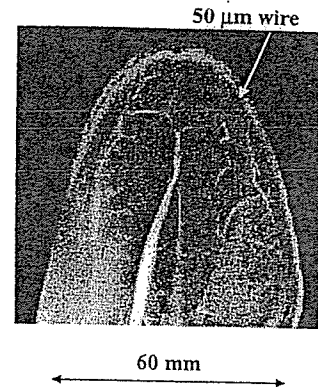


Fig. 10. Angiograms of external ear of rabbit.

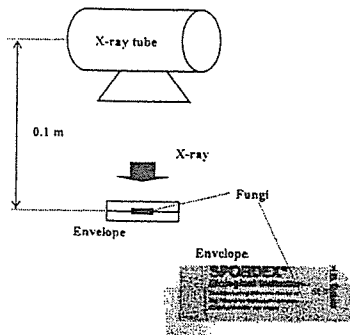


Fig. 11. Experimental setup for disinfection.

Table 1. Disinfection test for Bacillus subtilis.

Exposure time (hour)	Culture time (day)			
	1	2	3	4
6	+	+	+	+
12	-	-	+	+
18	-	-	-	-
24	-	-	-	-

Table 2. Disinfection test for staphylococcus.

Exposure time (hour)	Culture time (day)			
	1	2	3	4
1	-	+	+	+
2	-	+	+	+
3	-	-	-	-
4	-	-	-	-

Table 3. Disinfection test for B-coli.

Exposure time (hour)	Culture time (day)			
	1	2	3	4
1	-	-	-	-
2	-	-	-	-
3	-	-	-	-
4	-	-	-	-

## 6. DISCUSSION

In the present work, we succeeded in generating extremely soft x rays using a 0.2 mm-thick beryllium window in conjunction with a tungsten target. By the calculation of bremsstrahlung x rays, x rays with energies higher than 2 keV are produced. However, it is very difficult to measure the x-ray dose because there are no dosimeters with constant energy sensitivities.

In radiography, the image quality hardened in response to increases in the thickness of the aluminum filter, because the low-photon-energy x rays of the spectra were absorbed easily by the filter. Using this x-ray generator, although K-series characteristic x rays of tungsten are not produced, due to the tube voltage, the photon energies of the characteristic x rays

can be selected by the target element.

In the disinfection, the distance between the x-ray source and fungi should be decreased as much as possible to decrease the absorbed x-ray dose by air. Subsequently, because the air is dissociated greatly, ion beams will also be a useful technique for the disinfection and the excluding of static electricity from semiconductor devices.

Because it is possible to produce low-photon-energy x rays and to perform extremely soft radiography and x-ray disinfection, and to exclude electricity, this system can be applied in various fields.

## ACKNOWLEDGMENTS

This work was supported by Grants-in-Aid for Scientific Research (13470154, 13877114, and 16591222) and Advanced Medical Scientific Research from MECSSST, Health and Labor Sciences Research Grants (RAMT-nano-001, RHGTEFB-genome-005 and RHGTEFB-saisei-003), Grants from Keiryō Research Foundation, The Promotion and Mutual Aid Corporation for Private Schools of Japan, Japan Science and Technology Agency (JST), and New Energy and Industrial Technology Development Organization (NEDO, Industrial Technology Research Grant Program in '03).

## REFERENCES

1. A. C. Thompson, H. D. Zeman, G. S. Brown, J. Morrison, P. Reiser, V. Padmanabahn, L. Ong, S. Green, J. Giacomini, H. Gordon and E. Rubenstein, "First operation of the medical research facility at the NSLS for coronary angiography," *Rev. Sci. Instrum.*, **63**, pp. 625-628, 1992.
2. H. Mori, K. Hyodo, E. Tanaka, M. U. Mohammed, A. Yamakawa, Y. Shinozaki, H. Nakazawa, Y. Tanaka, T. Sekka, Y. Iwata, S. Honda, K. Umetani, H. Ueki, T. Yokoyama, K. Tanioka, M. Kubota, H. Hosaka, N. Ishizawa and M. Ando, "Small-vessel radiography in situ with monochromatic synchrotron radiation," *Radiology*, **201**, pp. 173-177, 1996.
3. K. Hyodo, M. Ando, Y. Oku, S. Yamamoto, T. Takeda, Y. Itai, S. Ohtsuka, Y. Sugishita and J. Tada, "Development of a two-dimensional imaging system for clinical applications of intravenous coronary angiography using intense synchrotron radiation produced by a multipole wiggler," *J. Synchrotron Rad.*, **5**, pp. 1123-1126, 1998.
4. T. J. Davis, D. Gao, T. E. Gureyev, A. W. Stevenson and S. W. Wilkims, "Phase-contrast imaging of weakly absorbing materials using hard x-rays," *Nature*, **373**, pp. 595-597, 1995.
5. A. Momose, T. Takeda, Y. Itai and K. Hirano, "Phase-contrast x-ray computed tomography for observing biological soft tissues," *Nature Medicine*, **2**, pp. 473-475, 1996.
6. M. Ando, A. Maksimenko, H. Sugiyama, W. Pattanasiriwisawa, K. Hyodo and C. Uyama, "A simple x-ray dark- and bright-field imaging using achromatic Laue optics," *Jpn. J. Appl. Phys.*, **41**, pp. L1016-L1018, 2002.
7. E. Sato, S. Kimura, S. Kawasaki, H. Isobe, K. Takahashi, Y. Tamakawa and T. Yanagisawa, "Repetitive flash x-ray generator utilizing a simple diode with a new type of energy-selective function," *Rev. Sci. Instrum.*, **61**, pp. 2343-2348, 1990.
8. E. Sato, M. Sagae, K. Takahashi, T. Oizumi, H. Ojima, K. Takayama, Y. Tamakawa, T. Yanagisawa, A. Fujiwara and K. Mitoya, "High-speed soft x-ray generators in biomedicine," *SPIE*, **2513**, pp. 649-667, 1994.
9. E. Sato, M. Sagae, K. Takahashi, A. Shikoda, T. Oizumi, H. Ojima, K. Takayama, Y. Tamakawa, T. Yanagisawa, A. Fujiwara and K. Mitoya, "Dual energy flash x-ray generator," *SPIE*, **2513**, pp. 723-735, 1994.
10. A. Shikoda, E. Sato, M. Sagae, T. Oizumi, Y. Tamakawa and T. Yanagisawa, "Repetitive flash x-ray generator having a high-durability diode driven by a two-cable-type line pulser," *Rev. Sci. Instrum.*, **65**, pp. 850-856, 1994.
11. E. Sato, K. Takahashi, M. Sagae, S. Kimura, T. Oizumi, Y. Hayasi, Y. Tamakawa and T. Yanagisawa, "Sub-kilohertz flash x-ray generator utilizing a glass-enclosed cold-cathode triode," *Med. & Biol. Eng. & Comput.*, **32**, pp. 289-294, 1994.
12. K. Takahashi, E. Sato, M. Sagae, T. Oizumi, Y. Tamakawa and T. Yanagisawa, "Fundamental study on a long-duration flash x-ray generator with a surface-discharge triode," *Jpn. J. Appl. Phys.*, **33**, pp. 4146-4151, 1994.
13. E. Sato, M. Sagae, A. Shikoda, K. Takahashi, T. Oizumi, M. Yamamoto, A. Takabe, K. Sakamaki, Y. Hayasi, H. Ojima, K. Takayama and Y. Tamakawa, "High-speed soft x-ray techniques," *SPIE*, **2869**, pp. 937-955, 1996.
14. E. Sato, Y. Hayasi, E. Tanaka, H. Mori, T. Kawai, T. Usuki, K. Sato, H. Obara, T. Ichimaru, K. Takayama, H. Ido and Y. Tamakawa, "Quasi-monochromatic radiography using a high-intensity quasi-x-ray laser generator," *SPIE*, **4682**, pp. 538-548, 2002.
15. E. Sato, Y. Hayasi, R. Germer, E. Tanaka, H. Mori, T. Kawai, H. Obara, T. Ichimaru, K. Takayama and H. Ido, "Intense characteristic x-ray irradiation from weakly ionized linear plasma and applications," *Jpn. J. Med. Imag. Inform. Sci.*, **20**, pp.

148-155, 2003.

16. E. Sato, Y. Hayasi, R. Germer, E. Tanaka, H. Mori, T. Kawai, H. Obara, T. Ichimaru, K. Takayama and H. Ido, "Irradiation of intense characteristic x-rays from weakly ionized linear molybdenum plasma," *Jpn. J. Med. Phys.*, **23**, pp. 123-131, 2003.

17. E. Sato, Y. Hayasi, R. Germer, E. Tanaka, H. Mori, T. Kawai, T. Ichimaru, K. Takayama and H. Ido, "Quasi-monochromatic flash x-ray generator utilizing weakly ionized linear copper plasma," *Rev. Sci. Instrum.*, **74**, pp. 5236-5240, 2003.

18. E. Sato, Y. Hayasi, R. Germer, E. Tanaka, H. Mori, T. Kawai, T. Ichimaru, S. Sato, K. Takayama and H. Ido, "Sharp characteristic x-ray irradiation from weakly ionized linear plasma," *J. Electron Spectroscopy and Related Phenomena*, **137-140**, pp. 713-720, 2004.

19. E. Sato, K. Sato and Y. Tamakawa, "Film-less computed radiography system for high-speed Imaging," *Ann. Rep. Iwate Med. Univ. Sch. Lib. Arts and Sci.*, **35**, pp. 13-23, 2000.

\*dresato@iwate-med.ac.jp; phone +81-19-651-5111; fax +81-19-654-9282

## Quasi-Monochromatic Flash X-Ray Generator Utilizing Disk-Cathode Molybdenum Tube

Eiichi SATO, Michiaki SAGAE, Etsuro TANAKA<sup>1</sup>, Yasuomi HAYASI, Rudolf GERMER<sup>2</sup>, Hidezo MORI<sup>3</sup>, Toshiaki KAWAI<sup>4</sup>, Toshio ICHIMARU<sup>5</sup>, Shigehiro SATO<sup>6</sup>, Kazuyoshi TAKAYAMA<sup>7</sup> and Hideaki IDO<sup>8</sup>

Department of Physics, Iwate Medical University, 3-16-1 Honchodori, Morioka 020-0015, Japan

<sup>1</sup>Department of Nutritional Science, Faculty of Applied Bio-science, Tokyo University of Agriculture, 1-1-1 Sakuragaoka, Setagaya-ku 156-8502, Japan

<sup>2</sup>ITP, FHTW FB1 and TU-Berlin, Blankenhainer Str. 9, D 12249 Berlin, Germany

<sup>3</sup>Department of Cardiac Physiology, National Cardiovascular Center Research Institute, 5-7-1 Fujishiro-dai, Suita, Osaka 565-8565, Japan

<sup>4</sup>Electron Tube Division #2, Hamamatsu Photonics Inc., 314-5 Shimokanzo, Toyooka Village, Iwata-gun 438-0193, Japan

<sup>5</sup>Department of Radiological Technology, School of Health Sciences, Hirosaki University, 66-1 Honcho, Hirosaki 036-8564, Japan

<sup>6</sup>Department of Microbiology, School of Medicine, Iwate Medical University, 19-1 Uchimarui, Morioka 020-8505, Japan

<sup>7</sup>Shock Wave Research Center, Institute of Fluid Science, Tohoku University, 2-1-1 Katahira, Aoba-ku, Sendai 980-8577, Japan

<sup>8</sup>Department of Applied Physics and Informatics, Faculty of Engineering, Tohoku Gakuin University, 1-13-1 Chuo, Tagajo 985-8537, Japan

(Received April 2, 2004; accepted June 14, 2004; published October 8, 2004)

High-voltage condensers in a polarity-inversion two-stage Marx surge generator are charged from  $-40$  to  $-60$  kV using a power supply, and the electric charges in the condensers are discharged to an X-ray tube after closing the gap switches in the surge generator using a trigger device. The X-ray tube is a demountable diode, and the turbomolecular pump evacuates air from the tube with a pressure of approximately 1 mPa. Sharp K-series characteristic X-rays of molybdenum are produced without using a monochromatic filter, since the tube utilizes a disk cathode and a rod target, and bremsstrahlung rays are not emitted in the opposite direction to that of electron acceleration. The peak tube voltage increased with increasing charging voltage and increasing space between the target and cathode electrodes. At a charging voltage of  $-60$  kV and a target-cathode space of 1.0 mm, the peak tube voltage and current were 110 kV and 0.75 kA, respectively. The pulse width ranged from 40 to 100 ns, and the maximum dimension of the X-ray source was 3.0 mm in diameter. The number of generator-produced K photons was approximately  $7 \times 10^{14}$  photons/cm<sup>2</sup>·s at 0.5 m from the source. [DOI: 10.1143/JJAP.43.7324]

KEYWORDS: flash X-ray, characteristic X-ray, quasi-monochromatic radiography, bremsstrahlung X-ray distribution

### 1. Introduction

Flash X-ray generators have been developed as a powerful tool in high-speed radiography because they produce extremely short X-ray pulses of less than 1  $\mu$ s. Currently, most generators utilize a multistage Marx surge generator<sup>1,2)</sup> in order to produce high-photon-energy flash X-rays by increasing the maximum tube voltage. On the other hand, soft flash X-ray generators<sup>3-7)</sup> with photon energies of less than 150 keV can be applied to biomedicine, and the repetition rate has been increased to the sub-kilohertz order.<sup>8)</sup>

High-dose-rate monochromatic X-rays are produced by a synchrotron in conjunction with single crystals and have been applied to X-ray phase imaging<sup>9,10)</sup> and microangiography.<sup>11)</sup> Subsequently, because extremely high-dose-rate quasi-monochromatic X-rays are produced from the axial direction of weakly ionized linear plasma,<sup>12-14)</sup> high-speed biomedical radiography has been performed. However, the bremsstrahlung X-rays are produced using targets of molybdenum, silver, cerium, and tungsten, since high-photon-energy bremsstrahlung X-rays are not absorbed effectively in the linear plasma. In addition, in cases where cold cathode triodes are employed, it is difficult to increase the condenser charging voltage to increase the photon energies of characteristic X-rays due to vacuum breakdown; the target voltage is equal to the charging voltage.

Because bremsstrahlung X-ray intensity varies with changes in the angle and direction of electron acceleration, characteristic X-rays are produced without using a monochromatic filter by selecting the irradiation direction. Although bremsstrahlung intensity is proportional to the atomic number, the angle selection will be a useful technique to produce quasi-monochromatic X-rays.

In this article, we describe a compact flash X-ray

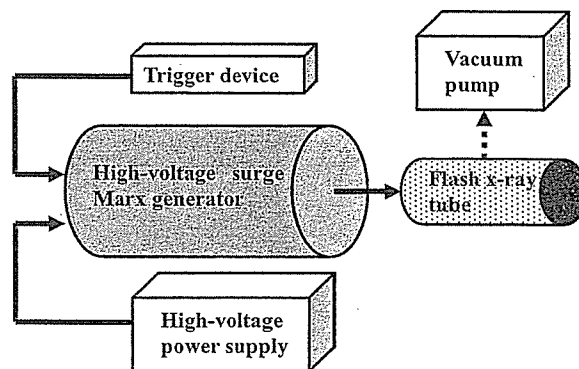


Fig. 1. Block diagram of compact quasi-monochromatic flash X-ray generator.

generator utilizing a molybdenum-target radiation tube, used to perform a preliminary experiment for generating quasi-monochromatic X-rays using the angle dependence of bremsstrahlung rays.

### 2. Generator

#### 2.1 High-voltage circuit

Figure 1 shows a block diagram of a compact quasi-monochromatic flash X-ray generator. This generator consists of the following components: a constant high-voltage power supply, a polarity-inversion two-stage surge Marx generator with a capacity during main discharge of 425 pF, a trigger device for the surge generator, a turbomolecular pump, and a flash X-ray tube. Since the electric circuit of the surge generator employs a polarity-inversion two-stage Marx line (Fig. 2), the surge produces twice the potential of the condenser charging voltage. When two condensers inside of the surge generator are charged from  $-40$  to

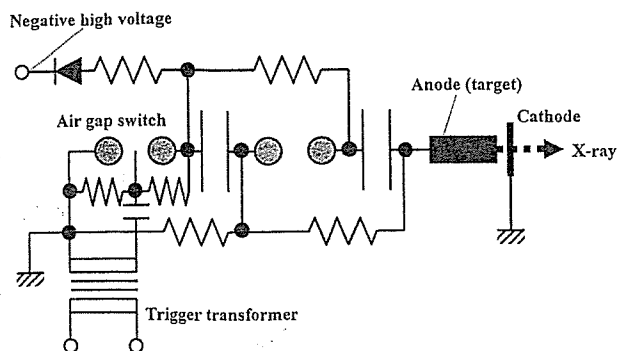


Fig. 2. Circuit diagram of flash X-ray generator.

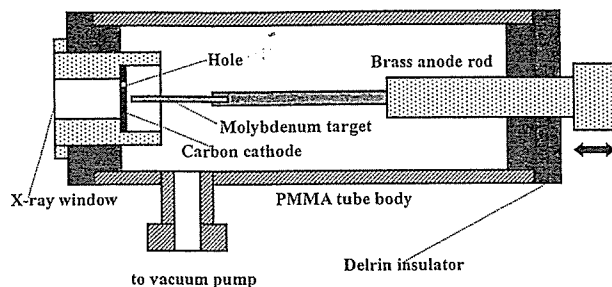


Fig. 3. Schematic drawing of flash X-ray tube.

-60 kV, the ideal output voltage ranges from 80 to 120 kV.

### 2.2 X-ray tube

The X-ray tube is of the demountable diode type, as illustrated in Fig. 3. This tube is connected to the turbomolecular pump with a pressure of approximately 1 mPa and consists of the following major devices: a rod-shaped molybdenum target, a disk cathode made of graphite, a polyethylene terephthalate (Mylar) X-ray window 0.25 mm in thickness, and a polymethyl methacrylate (PMMA) tube body. The target-cathode (T-C) space was regulated from the outside of the X-ray tube by rotating the anode rod, and

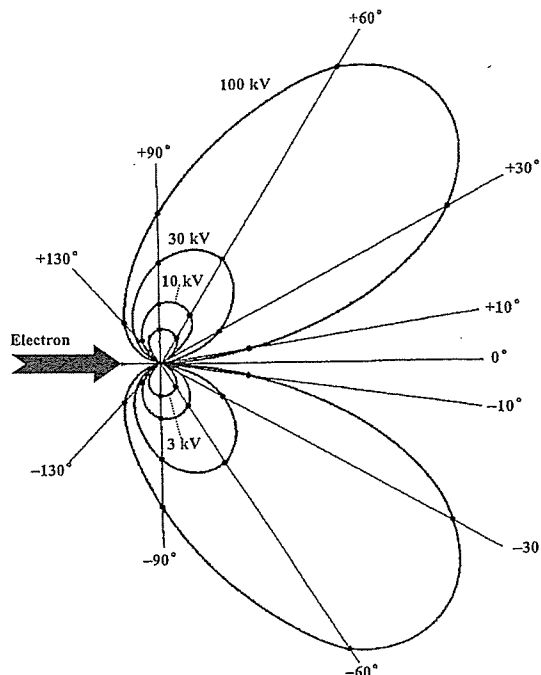


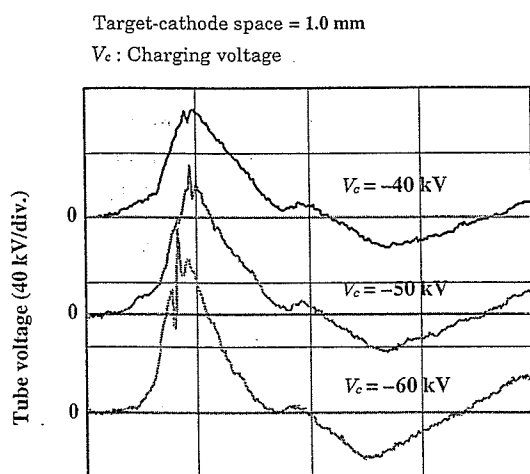
Fig. 4. Bremsstrahlung X-ray intensity distribution vs angle.

the transmission X-rays are obtained through a 1.0 mm-thick graphite cathode and an X-ray window. Because bremsstrahlung rays are not emitted in the opposite direction to that of electron acceleration (Fig. 4), characteristic X-rays can be produced.

### 3. Characteristics

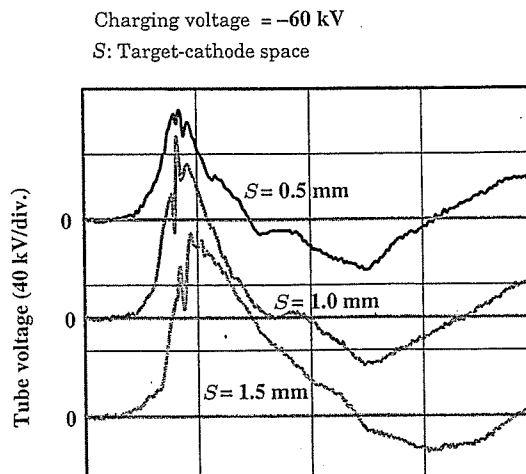
#### 3.1 Tube voltage and current

Tube voltage and current were measured using a high-voltage divider with an input impedance of 10 kΩ and a current transformer, respectively (Figs. 5 and 6). The voltage and current roughly displayed damped oscillations. At a constant T-C space of 1.0 mm, peak voltage increased slightly with increasing charging voltage. In contrast, peak



Time (100 ns/div.)

(a)



Time (100 ns/div.)

(b)

Fig. 5. Variations in tube voltage with changes in (a) charging voltage and (b) space.

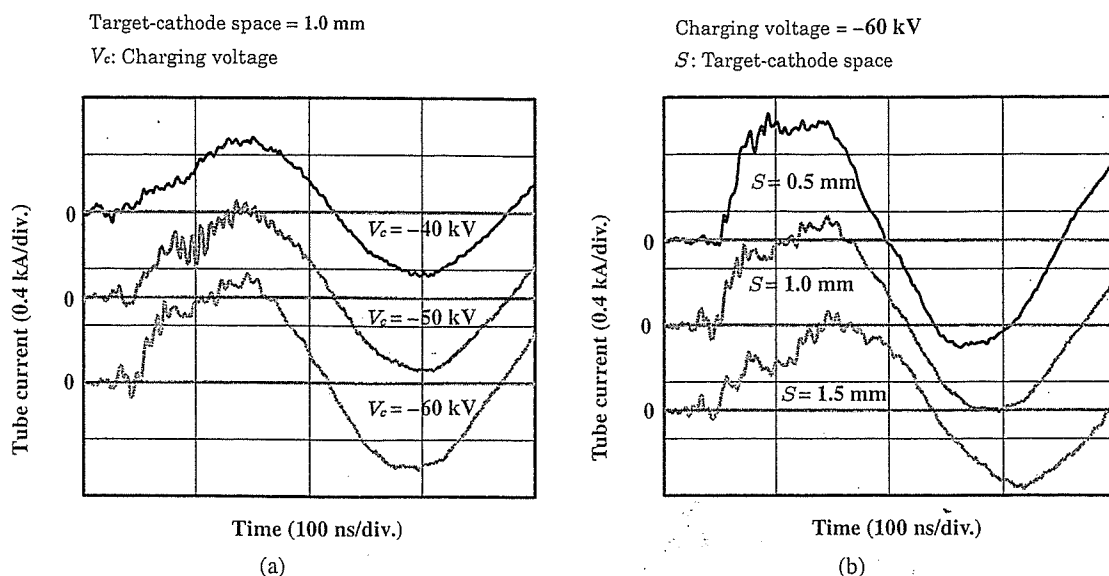


Fig. 6. Tube currents with changes in (a) charging voltage and (b) space.

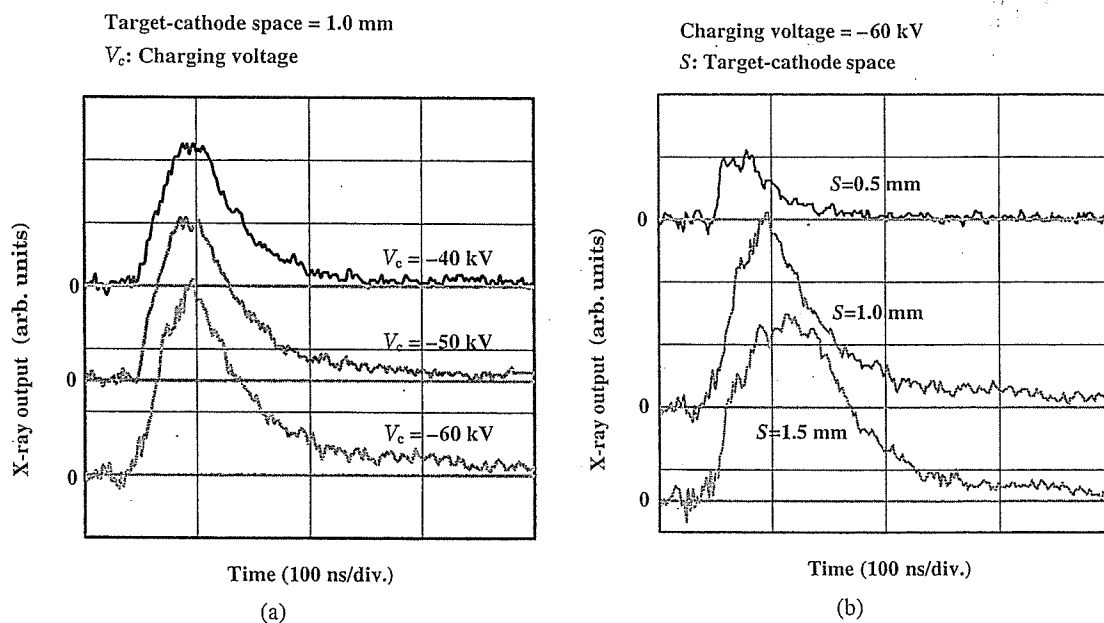


Fig. 7. X-ray outputs according to changes in (a) charging voltage and (b) space.

voltage substantially increased when T-C space was increased at a constant charging voltage of  $-60$  kV. Subsequently, peak tube current increased with increasing charging voltage. When T-C space was increased, current rise time increased, and peak current decreased. At a charging voltage of  $-60$  kV and a T-C space of  $1.0$  mm, peak tube voltage and current were  $110$  kV and  $0.75$  kA, respectively.

### 3.2 X-ray output

X-ray output pulse was detected using a combination of a plastic scintillator and a photomultiplier (Fig. 7). When the charging voltage was increased, the pulse height increased, but the width seldom varied. Next, with increases in the T-C space, the height was maximized, and the width increased. In the present work, the width ranged from  $40$  to  $100$  ns. Next,

the time-integrated X-ray intensity measured using a thermoluminescence dosimeter (Kyokko TLD Reader 1500 having MSO-S elements without energy compensation) was approximately  $3.0 \mu\text{C}/\text{kg}$  at  $0.5$  m from the X-ray source with a charging voltage of  $-60$  kV and a T-C space of  $1.0$  mm.

### 3.3 X-ray source

In order to measure the images of the X-ray source, we employed a pinhole camera with a hole diameter of  $100 \mu\text{m}$  (Fig. 8). When the charging voltage was increased, the plasma X-ray source grew, and both spot dimension and intensity increased. The maximum dimension was almost equal to the target diameter and had a value of approximately  $3.0$  mm.



$V_c$ : Charging voltage

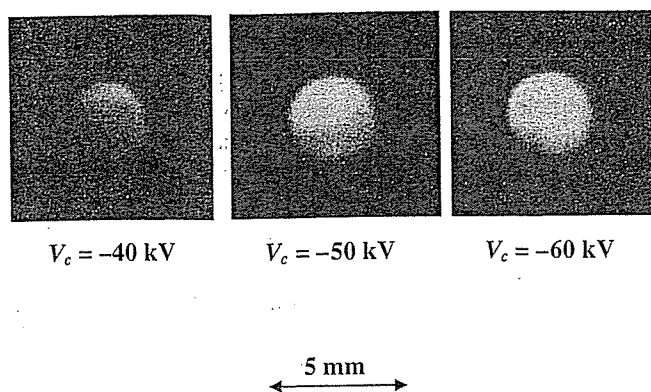


Fig. 8. Images of X-ray source with changes in charging voltage at constant space between target and cathode electrodes.

3.4 X-ray spectra

X-ray spectra were measured by a transmission-type spectrometer with a lithium fluoride curved crystal 0.5 mm in thickness. The spectra were measured using a computed radiography (CR) system<sup>15)</sup> (Konica Regius 150) with a wide dynamic range, and relative X-ray intensity was calculated from Dicom digital data. Figure 9 shows the measured spectra from the molybdenum target. We observed sharp lines of K-series characteristic X-rays, while bremsstrahlung rays were hardly detected. The characteristic X-ray intensity of the  $K\alpha$  and  $K\beta$  lines substantially increased with increasing charging voltage.

4. Radiography

Flash radiography was performed using the CR system at 0.5 m from the X-ray source, and the charging voltage and the T-C space were  $-60$  kV and 1.0 mm, respectively.

Firstly, rough measurements of spatial resolution were made using wires. Figure 10 shows radiograms of tungsten wires coiled around a pipe made of polymethyl methacry-

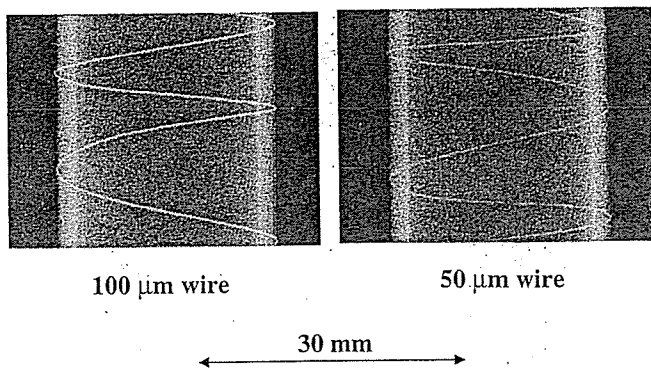


Fig. 10. Radiograms of tungsten wires of 50 and 100 μm in diameter coiled around pipes made of polymethyl methacrylate.

late. Although the image contrast increased with increasing wire diameter, a 50-μm-diameter wire could be observed.

An image of plastic bullets falling into a polypropylene beaker from a glass test tube is shown in Fig. 11. Because the X-ray pulse widths were approximately 60 ns, the stop-motion image of bullets could be obtained. Figure 12 shows an angiogram of a rabbit heart; iodine-based microspheres of 15 μm in diameter were used, and fine blood vessels of approximately 100 μm were visible.

5. Discussion

Concerning the spectrum measurement, sharp molybdenum K-series characteristic X-rays were obtained, and monochromatic  $K\alpha$  lines can be obtained using a zirconium filter. The photon energies of characteristic X-rays are determined by the target element, and the X-ray intensity increases with increasing tube voltage by increasing the charging voltage. As compared with the plasma flash X-ray generator utilizing a molybdenum target triode,<sup>13)</sup> bremsstrahlung X-rays were hardly observed at all even when higher tube voltages were applied to the diode, since the characteristic X-rays were produced from the target tip. Because the maximum tube voltage can be increased easily, and high-photon-energy K-series characteristic X-rays from

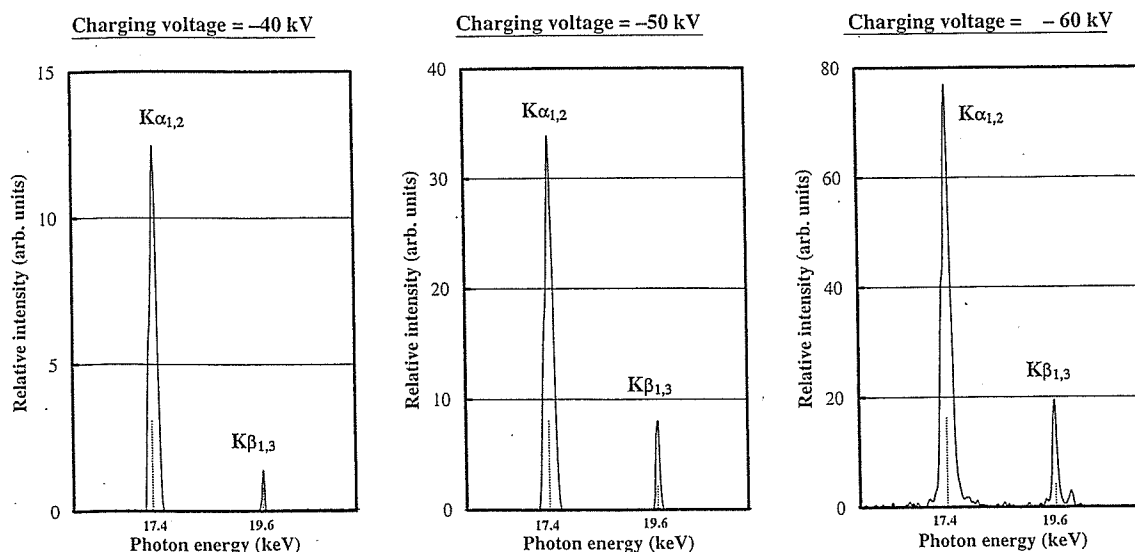
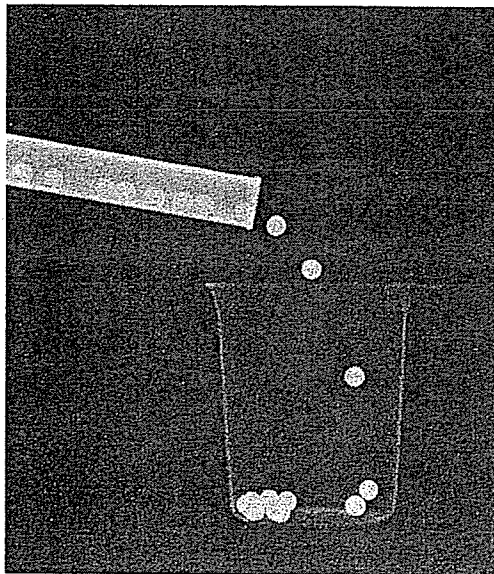


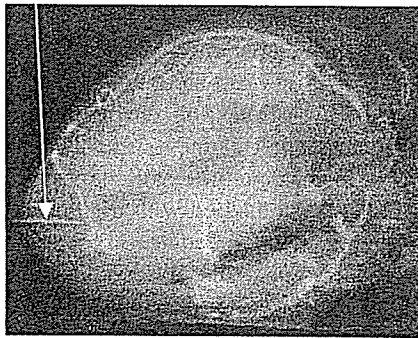
Fig. 9. X-ray spectra from weakly ionized molybdenum plasma according to changes in charging voltage with space of 1.0 mm.



50 mm

Fig. 11. Radiograms of plastic bullets falling into polypropylene beaker from glass test tube.

100  $\mu\text{m}$  tungsten wire



30 mm

Fig. 12. Angiogram of rabbit heart.

the cerium or tungsten target can be produced. In particular, the cerium target is very useful in order to perform microangiography using iodine-based contrast mediums.

In this research, although the number of generator-produced characteristic K photons was approximately  $7 \times 10^{14}$  photons/cm<sup>2</sup>·s at 0.5 m from the source, the number can be increased easily by increasing the electrostatic energy in the condensers.

Using this generator, because the photon energies of characteristic X-rays can be selected, various quasi-monochromatic high-speed radiographies, such as high contrast microangiography and photon-counting radiography for decreasing noise from radiograms, will be possible.

#### Acknowledgment

This work was supported by Grants-in-Aid for Scientific Research (13470154, 13877114, and 16591222) and Advanced Medical Scientific Research from MECSSST, Grants from Keiryō Research Foundation, JST (Test of Fostering Potential), NEDO, and MHLW (HLSRG, RAMT-nano-001, RHGTEFB-genome-005, and RGCD13C-1).

- 1) A. Mattsson: *Physica Scripta* **5** (1972) 99.
- 2) R. Germer: *J. Phys. E: Sci. Instrum.* **12** (1979) 336.
- 3) E. Sato, H. Isobe and F. Hoshino: *Rev. Sci. Instrum.* **57** (1986) 1399.
- 4) E. Sato, M. Sagae, K. Takahashi, A. Shikoda, T. Oizumi, Y. Hayasi, Y. Tamakawa and T. Yanagisawa: *Med. & Biol. Eng. & Comput.* **32** (1994) 295.
- 5) A. Shikoda, E. Sato, M. Sagae, T. Oizumi, Y. Tamakawa and T. Yanagisawa: *Rev. Sci. Instrum.* **65** (1994) 850.
- 6) E. Sato, M. Sagae, A. Shikoda, K. Takahashi, T. Oizumi, M. Yamamoto, A. Takabe, K. Sakamaki, Y. Hayasi, H. Ojima, K. Takayama and Y. Tamakawa: *Proc. SPIE* **2869** (1996) 937.
- 7) K. Takahashi, E. Sato, M. Sagae, T. Oizumi, Y. Tamakawa and T. Yanagisawa: *Jpn. J. Appl. Phys.* **33** (1994) 4146.
- 8) E. Sato, K. Takahashi, M. Sagae, S. Kimura, T. Oizumi, Y. Hayasi, Y. Tamakawa and T. Yanagisawa: *Med. & Biol. Eng. & Comput.* **32** (1994) 289.
- 9) T. J. Davis, D. Gao, T. E. Gureyev, A. W. Stevenson and S. W. Wilkims: *Nature* **373** (1995) 595.
- 10) A. Momose, T. Takeda, Y. Itai and K. Hirano: *Nature Medicine* **2** (1996) 473.
- 11) H. Mori *et al.*: *Radiology* **201** (1996) 173.
- 12) E. Sato, Y. Hayasi, R. Germer, E. Tanaka, H. Mori, T. Kawai, H. Obara, T. Ichimaru, K. Takayama and H. Ido: *Jpn. J. Med. Imag. Inform. Sci.* **20** (2003) 148.
- 13) E. Sato, Y. Hayasi, R. Germer, E. Tanaka, H. Mori, T. Kawai, H. Obara, T. Ichimaru, K. Takayama and H. Ido: *Jpn. J. Med. Phys.* **23** (2003) 123.
- 14) E. Sato, Y. Hayasi, R. Germer, E. Tanaka, H. Mori, T. Kawai, T. Ichimaru, K. Takayama and Hideaki Ido: *Rev. Sci. Instrum.* **74** (2003) 5236.
- 15) E. Sato, K. Sato and Y. Tamakawa: *Ann. Rep. Iwate Med. Univ. Sch. Lib. Arts and Sci.* **35** (2000) 13.

# Demonstration of enhanced *K*-edge angiography using a cerium target x-ray generator

Eiichi Sato<sup>a)</sup>

*Department of Physics, Iwate Medical University, Morioka 020-0015, Japan*

Etsuro Tanaka

*Department of Nutritional Science, Faculty of Applied Bio-science, Tokyo University of Agriculture, Setagayaku 156-8502, Japan*

Hidezo Mori

*Department of Cardiac Physiology, National Cardiovascular Center Research Institute, Osaka 565-8565, Japan*

Toshiaki Kawai

*Electron Tube Division #2, Hamamatsu Photonics Inc., Iwata-gun 438-0193, Japan*

Toshio Ichimaru

*Department of Radiological Technology, School of Health Sciences, Hirosaki University, Hirosaki 036-8564, Japan*

Shigehiro Sato

*Department of Microbiology, School of Medicine, Iwate Medical University, Morioka 020-8505, Japan*

Kazuyoshi Takayama

*Shock Wave Research Center, Institute of Fluid Science, Tohoku University, Sendai 980-8577, Japan*

Hideaki Ido

*Department of Applied Physics and Informatics, Faculty of Engineering, Tohoku Gakuin University, Tagajo 985-8537, Japan*

(Received 18 May 2004; revised 8 July 2004; accepted for publication 14 August 2004; published 22 October 2004)

The cerium target x-ray generator is useful in order to perform enhanced *K*-edge angiography using a cone beam because *K*-series characteristic x rays from the cerium target are absorbed effectively by iodine-based contrast mediums. The x-ray generator consists of a main controller, a unit with a Cockcroft-Walton circuit and a fixed anode x-ray tube, and a personal computer. The tube is a glass-enclosed diode with a cerium target and a 0.5-mm-thick beryllium window. The maximum tube voltage and current were 65 kV and 0.4 mA, respectively, and the focal-spot sizes were 1.0 × 1.3 mm. Cerium *K* $\alpha$  lines were left using a barium sulfate filter, and the x-ray intensity was 0.48  $\mu\text{C}/\text{kg}$  at 1.0 m from the source with a tube voltage of 60 kV, a current of 0.40 mA, and an exposure time of 1.0 s. Angiography was performed with a computed radiography system using iodine-based microspheres. In coronary angiography of nonliving animals, we observed fine blood vessels of approximately 100  $\mu\text{m}$  with high contrasts. © 2004 American Association of Physicists in Medicine. [DOI: 10.1118/1.1803433]

Key words: x-ray source, x-ray tube, x-ray spectra, attenuation coefficient, angiography

## I. INTRODUCTION

Synchrotrons generate monochromatic parallel x-ray beams using single crystals. These beams with photon energies of approximately 35 keV have been employed to perform enhanced *K*-edge angiography,<sup>1-4</sup> since the beams are absorbed effectively by iodine-based contrast mediums. However, it is difficult to increase the irradiation field, due to the parallel beam, and to obtain sufficient machine times for various research projects, including medical applications.

Currently, flash x-ray generators utilize cold-cathode radiation tubes and produce extremely short x-ray pulses of less than 1  $\mu\text{s}$ . So far, several different flash x-ray generators have been developed,<sup>5</sup> and the generators with photon energies of lower than 150 keV<sup>6-11</sup> can be employed to perform

biomedical radiography. In order to produce monochromatic x rays, plasma flash x-ray generators are useful, since quite intense and clean characteristic x rays have been produced from weakly ionized linear plasmas of nickel, copper,<sup>12</sup> and molybdenum,<sup>13</sup> while bremsstrahlung rays are hardly detected at all. Using these generators, the characteristic x-ray intensity substantially increased with corresponding increases in the charging voltage.

Since *K*-series characteristic x rays from cerium target are absorbed effectively by iodine-based contrast mediums, a cerium-target x-ray tube is very useful in order to perform high contrast angiography. On the other hand, cerium is a rare earth element and has a high reactivity, and it is difficult to design the target. However, we are very interested in pro-

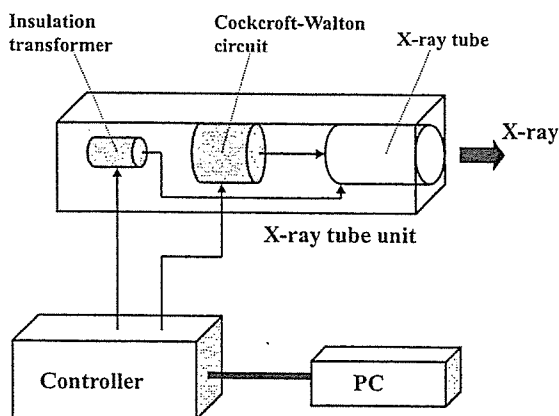


FIG. 1. Block diagram of the compact x-ray generator with a cerium-target radiation tube, which is used specially for  $K$ -edge angiography using iodine-based contrast mediums.

ducing cerium characteristic x rays to perform cone beam angiography because the irradiation field can be increased easily.

In the present research, we developed a compact x-ray generator with a cerium target tube, and used it to perform a preliminary study on enhanced  $K$ -edge angiography achieved with cerium  $K\alpha$  rays.

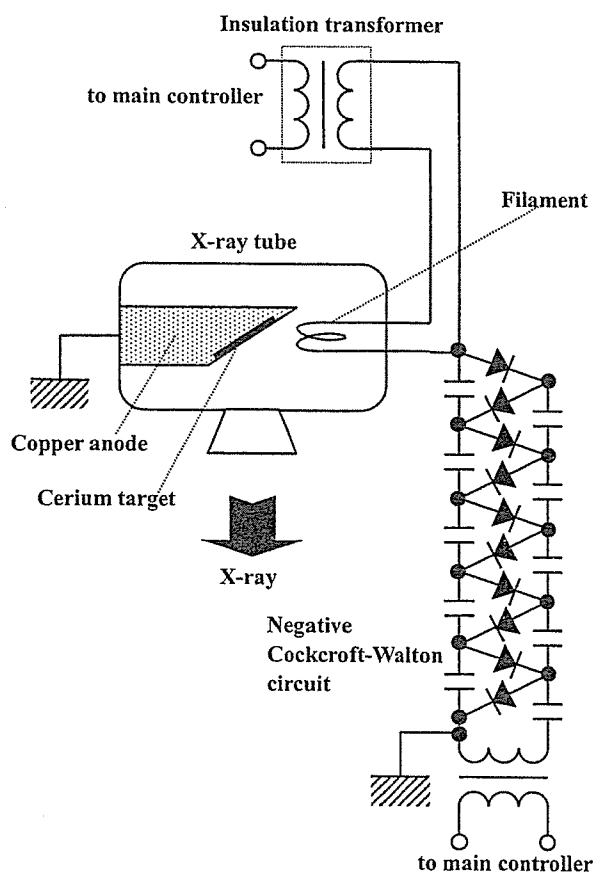


FIG. 2. Main circuit of the x-ray generator.

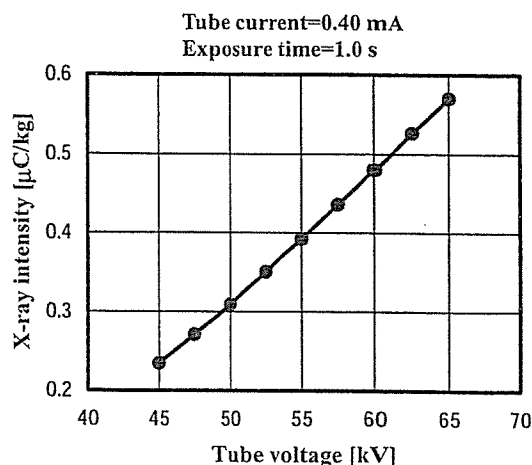


FIG. 3. X-ray intensity measured at 1.0 m from the x-ray source according to changes in the tube voltage.

## II. GENERATOR

Figure 1 shows the block diagram of the x-ray generator, which consists of a main controller, an x-ray tube unit with a Cockcroft-Walton circuit, and a cerium-target tube, and a personal computer. The tube voltage, the current, and the exposure time can be controlled by both the controller and the computer. The main circuit for producing x rays is illustrated in Fig. 2, and employed the Cockcroft-Walton circuit in order to decrease the dimensions of the tube unit. In the circuit, the condensers are always in series, and are charged serially. In the x-ray tube, the negative high voltage is applied to the cathode electrode, and the anode (target) is connected to the tube unit case (ground potential) to cool the anode and the target effectively. The filament heating current is supplied by an ac power supply in the controller in conjunction with an insulation transformer which is used for isolation from the high voltage from the Cockcroft-Walton circuit. In this experiment, the tube voltage applied was from 45 to 65 kV, and the tube current was regulated to within 0.40 mA (maximum current) by the filament temperature. The exposure time is controlled in order to obtain optimum x-ray intensity. Monochromatic  $K\alpha$  lines were left using a 5-mm-thick barium sulfate filter in which barium sulfate powder was mixed with polymethyl methacrylate (PMMA) resin, since both the bremsstrahlung and the  $K\beta$  rays were absorbed effectively by the filter. In designing the filter, the surface density of the barium sulfate powder is important, since the x rays are absorbed effectively by the powder as compared with the PMMA resin. In this case, the density was  $7.6 \text{ mg}/\text{cm}^2$ .

## III. CHARACTERISTICS

### A. X-ray intensity

X-ray intensity was measured by a Victoreen 660 ionization chamber at 1.0 m from the x-ray source using the filter with an exposure time of 1.0 s (Fig. 3). At a constant tube current of 0.40 mA, the x-ray intensity increased when the tube voltage was increased. In this measurement, the inten-

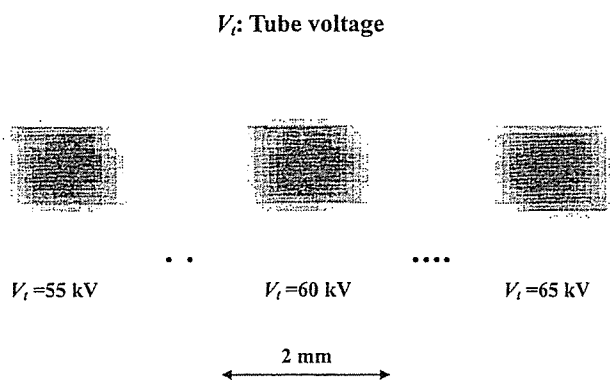


FIG. 4. Effective focal spots with changes in the tube voltage.

sity with a tube voltage of 60 kV and a current of 0.40 mA was  $0.48 \mu\text{C}/\text{kg}$  at 1.0 m from the source with errors of less than 0.2%.

### B. Focal spot

In order to measure images of the x-ray source after the barium sulfate filtration, we employed a pinhole camera with a hole diameter of  $50 \mu\text{m}$  (magnification ratio of 1:1) in conjunction with a computed radiography (CR) system<sup>14,15</sup> with a sampling pitch of  $87.5 \mu\text{m}$ . When the tube voltage was increased, spot dimensions seldom varied and had values of  $1.0 \times 1.3 \text{ mm}$  (Fig. 4).

### C. X-ray spectra

In order to measure x-ray spectra, we employed a cadmium tellurium detector (CDTE2020X, Hamamatsu Photonics Inc.) (Fig. 5). Compared with a germanium detector, this detector has a lower energy resolution of 1.7 keV. When the tube voltage was increased, the characteristic x-ray intensities of  $K\alpha$  lines increased, and both the maximum photon energy and the intensities of bremsstrahlung x rays increased. The barium sulfate filter significantly attenuate the spectra above the barium  $K$ -edge energy of 37.399 keV. The areas under the spectral curves correlate closely to the total x-ray intensities shown in Fig. 3.

## IV. ANGIOGRAPHY

Figure 6 shows the mass attenuation coefficients of iodine at the selected energies; the coefficient curve is discontinuous at the iodine  $K$  edge. The average photon energy of the cerium  $K\alpha$  lines is shown just above the iodine  $K$  edge. Cerium is a rare earth element and has a high reactivity; however, the average photon energy of  $K\alpha$  lines is 34.566 keV, and iodine contrast mediums with a  $K$ -absorption edge of 33.155 keV absorb the lines easily. Therefore, blood vessels were observed with high contrasts. Subsequently, in angiography testing, we usually employ nonliving animal phantoms using microspheres.

The angiography was performed by the CR system (Konica Regius 150) using the filter, and the distance (between the x-ray source and the imaging plate) was 1.5 m.

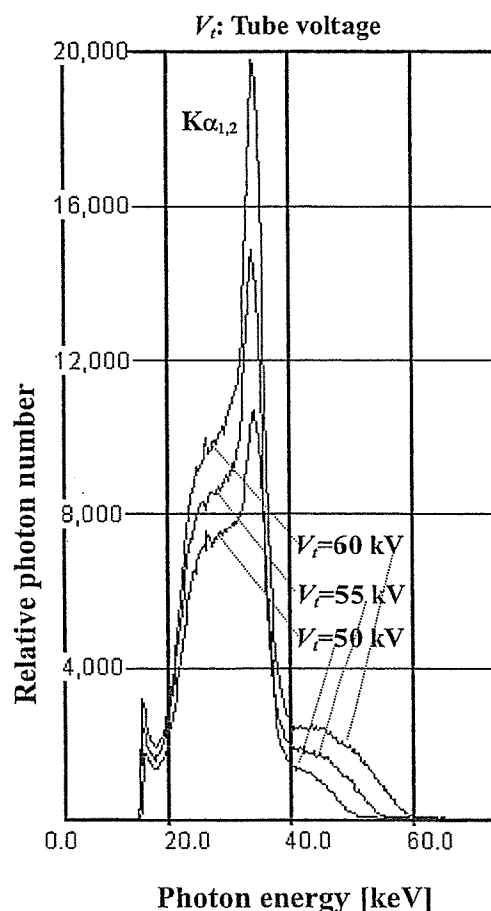


FIG. 5. X-ray spectra measured by a cadmium tellurium detector with changes in the tube voltage.

First, rough measurements of image resolution were made using wires. Figure 7 shows radiograms of tungsten wires in a rod made of PMMA with a tube voltage of 60 kV. Although the image contrast decreased somewhat with decreases in the wire diameter, due to blurring of the image caused by the sampling pitch of  $87.5 \mu\text{m}$ , a  $50\text{-}\mu\text{m}$ -diameter wire could be observed.

Angiograms of rabbit hearts are shown in Fig. 8. These two images were obtained using iodine and cerium micro-

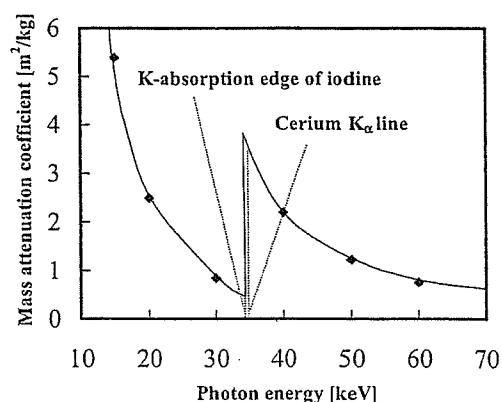


FIG. 6. Mass attenuation coefficients of iodine, and the average photon energy of the cerium  $K\alpha$  lines is shown just above the iodine  $K$  edge.

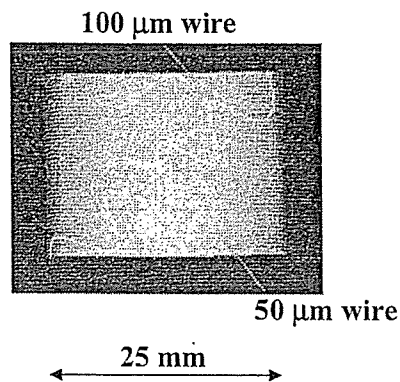


FIG. 7. Radiograms of tungsten wires in a PMMA rod with a tube voltage of 60 kV.

spheres of 15  $\mu\text{m}$  in diameter at a tube voltage of 60 kV. The iodine spheres contained 37% iodine by weight, and the cerium spheres contained 18% cerium by weight. The concentration of spheres in the blood varies with the filling rate, and the estimated densities of the iodine and the cerium of blood are less than 0.44 and 0.17  $\text{g}/\text{cm}^3$ , respectively. In the case where the cerium spheres were employed, the coronary arteries were barely visible. Figure 9(a) shows an angiogram of a larger dog heart using the cerium target at a tube voltage of 60 kV using iodine spheres. For comparison, we performed angiography with a tungsten x-ray tube at a tube voltage of 60 kV [Fig. 9(b)].

If we assume that the filling rate of the iodine microspheres in a blood vessel is constant, the image contrast of the blood is in inverse proportion to the vessel diameter. Next, the density ratios (maximum density divided by minimum density) obtained by the cerium and tungsten tubes were 4.3 and 2.7, respectively. In angiography using the tungsten target, blood vessels of approximately 100  $\mu\text{m}$  were hardly observed at all.

## V. DISCUSSION

In summary, we developed a x-ray generator with a cerium-target tube and succeeded in producing cerium  $K\alpha$  lines, which can be absorbed easily by iodine-based contrast mediums. Both the characteristic and bremsstrahlung x-ray

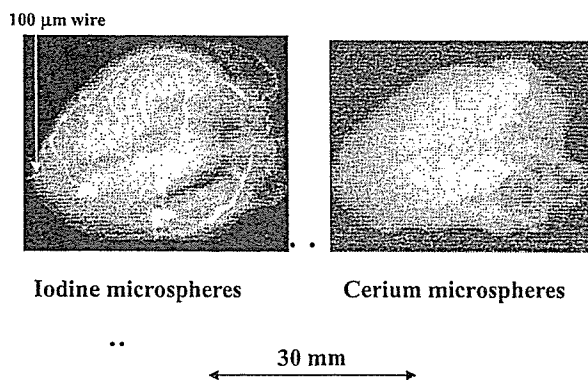


FIG. 8. Angiograms of extracted rabbit hearts using iodine and cerium microspheres with a tube voltage of 60 kV.

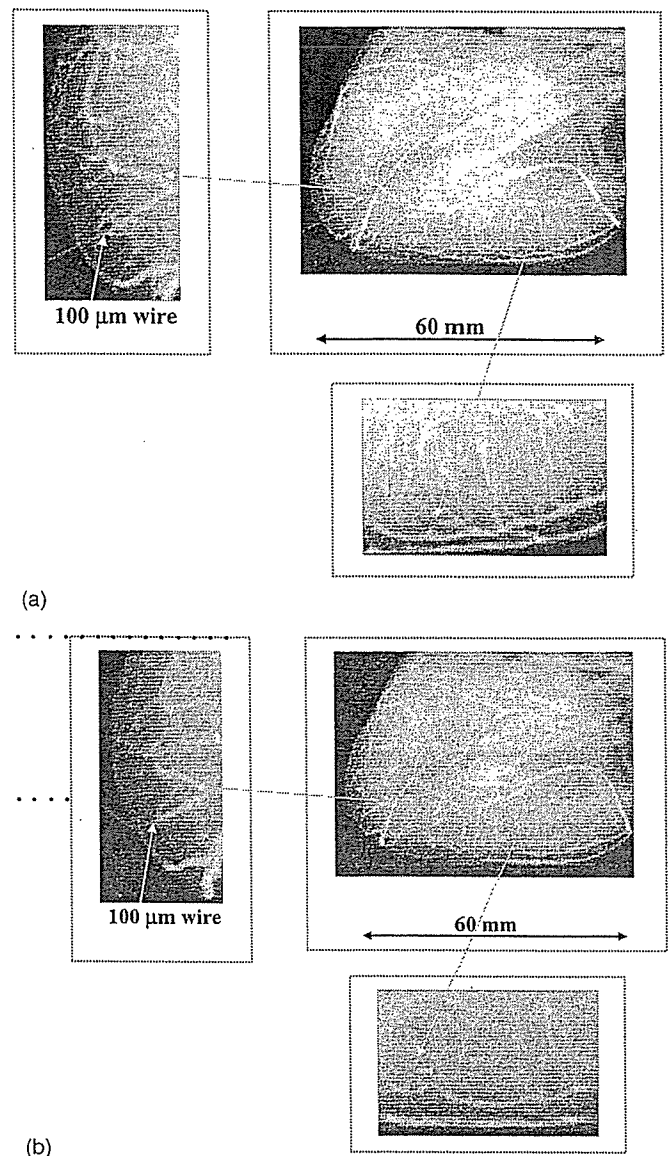


FIG. 9. Angiograms of an extracted dog heart achieved with (a) cerium and (b) tungsten target x-ray tubes using iodine microspheres with a tube voltage of 60 kV.

intensities increased with increases in the tube voltage, and  $K\beta$  lines were absorbed effectively by the barium sulfate filter. The x-ray intensity was limited because the thermal contact between the target and the anode was not good. However, the intensity can be increased by welding the target or using a cerium-alloy target.

In this preliminary experiment, although the maximum tube voltage and current were 65 kV and 0.40 mA, respectively, the voltage and current could be increased. Subsequently, the generator produced maximum number of characteristic photons was approximately  $3 \times 10^7$  photons/ $\text{cm}^2 \text{ s}$  at 1.0 m from the source, and the photon count rate can be increased easily by improving the target.

Since the sampling pitch of the CR system is 87.5  $\mu\text{m}$ , we obtained resolutions of approximately 100  $\mu\text{m}$ , and high-contrast blood vessels could be observed using a CR system. In order to observe fine blood vessels of less than 100  $\mu\text{m}$ ,

the image resolution of the CR system should be improved as much as possible, and a flat panel system is useful to observe blood flows for cases of cardiovascular disease.

## ACKNOWLEDGMENTS

This work was supported by Grants-in-Aid for Scientific Research and Advanced Medical Scientific Research from MECSS (13470154, 13877114, and 16591222), Grants from Keiryō Research Foundation, JST (Test of Fostering Potential), NEDO, and MHLW (HLSRG, RAMT-nano-001, RHGTEFB-genome-005, and RGCD13C-1).

<sup>3</sup>Author to whom correspondence should be addressed. Department of Physics, Iwate Medical University, 3-16-1 Honchodori, Morioka 020-0015, Japan; electronic mail: dresato@iwate-med.ac.jp

<sup>1</sup>A. Akisada, M. Ando, K. Hyodo, S. Hasegawa, K. Konishi, K. Nishimura, A. Maruhashi, F. Toyofuku, A. Suwa, and K. Kohra, "An attempt at coronary angiography with a large size monochromatic SR beam," *Nucl. Instrum. Methods Phys. Res. A* **246**, 713–718 (1986).

<sup>2</sup>A. C. Thompson, H. D. Zeman, G. S. Brown, J. Morrison, P. Reiser, V. Padmanabahn, L. Ong, S. Green, J. Giacomini, H. Gordon, and E. Rubenstein, "First operation of the medical research facility at the NSLS for coronary angiography," *Rev. Sci. Instrum.* **63**, 625–628 (1992).

<sup>3</sup>H. Mori, K. Hyodo, E. Tanaka, M. U. Mohammed, A. Yamakawa, Y. Shinozaki, H. Nakazawa, Y. Tanaka, T. Sekka, Y. Iwata, S. Honda, K. Umetani, H. Ueki, T. Yokoyama, K. Tanioka, M. Kubota, H. Hosaka, N. Ishizawa, and M. Ando, "Small-vessel radiography in situ with monochromatic synchrotron radiation," *Radiology* **201**, 173–177 (1996).

<sup>4</sup>K. Hyodo, M. Ando, Y. Oku, S. Yamamoto, T. Takeda, Y. Itai, S. Ohtsuka, Y. Sugishita, and J. Tada, "Development of a two-dimensional imaging system for clinical applications of intravenous coronary angiography using intense synchrotron radiation produced by a multipole wiggler," *J. Synchrotron Radiat.* **5**, 1123–1126 (1998).

<sup>5</sup>R. Germer, "X-ray flash techniques," *J. Phys. E* **12**, 336–350 (1979).

<sup>6</sup>E. Sato, H. Isobe, and F. Hoshino, "High intensity flash x-ray apparatus for biomedical radiography," *Rev. Sci. Instrum.* **57**, 1399–1408 (1986).

<sup>7</sup>E. Sato, S. Kimura, S. Kawasaki, H. Isobe, K. Takahashi, Y. Tamakawa, and T. Yanagisawa, "Repetitive flash x-ray generator utilizing a simple diode with a new type of energy-selective function," *Rev. Sci. Instrum.* **61**, 2343–2348 (1990).

<sup>8</sup>A. Shikoda, E. Sato, M. Sagae, T. Oizumi, Y. Tamakawa, and T. Yanagisawa, "Repetitive flash x-ray generator having a high-durability diode driven by a two-cable-type line pulser," *Rev. Sci. Instrum.* **65**, 850–856 (1994).

<sup>9</sup>E. Sato, K. Takahashi, M. Sagae, S. Kimura, T. Oizumi, Y. Hayasi, Y. Tamakawa, and T. Yanagisawa, "Sub-kilohertz flash x-ray generator utilizing a glass-enclosed cold-cathode triode," *Med. Biol. Eng. Comput.* **32**, 289–294 (1994).

<sup>10</sup>K. Takahashi, E. Sato, M. Sagae, T. Oizumi, Y. Tamakawa, and T. Yanagisawa, "Fundamental study on a long-duration flash x-ray generator with a surface-discharge triode," *Jpn. J. Appl. Phys., Part 1* **33**, 4146–4151 (1994).

<sup>11</sup>E. Sato, M. Sagae, K. Takahashi, A. Shikoda, T. Oizumi, Y. Hayasi, Y. Tamakawa, and T. Yanagisawa, "10 kHz microsecond pulsed x-ray generator utilizing a hot-cathode triode with variable durations for biomedical radiography," *Med. Biol. Eng. Comput.* **32**, 295–301 (1994).

<sup>12</sup>E. Sato, Y. Hayasi, R. Germer, E. Tanaka, H. Mori, T. Kawai, T. Ichimaru, K. Takayama, and H. Ido, "Quasi-monochromatic flash x-ray generator utilizing weakly ionized linear copper plasma," *Rev. Sci. Instrum.* **74**, 5236–5240 (2003).

<sup>13</sup>E. Sato, Y. Hayasi, R. Germer, E. Tanaka, H. Mori, T. Kawai, H. Obara, T. Ichimaru, K. Takayama, and H. Ido, "Irradiation of intense characteristic x-rays from weakly ionized linear molybdenum plasma," *Jpn. J. Med. Phys.* **23**, 123–131 (2003).

<sup>14</sup>M. Sonoda, M. Takano, J. Miyahara, and H. Kato, "Computed radiography utilizing scanning laser stimulated luminescence," *Radiology* **148**, 833–838 (1983).

<sup>15</sup>E. Sato, K. Sato, and Y. Tamakawa, "Film-less computed radiography system for high-speed imaging," *Ann. Rep. Iwate Med. Univ. Sch. Lib. Arts and Sci.* **35**, 13–23 (2000).

## Bremsstrahlung X-ray Spectra for Enhanced K-edge Angiography

Eiichi Sato<sup>a</sup>, Etsuro Tanaka<sup>b</sup>, Hidezo Mori<sup>c</sup>, Toshiaki Kawai<sup>d</sup>, Toshio Ichimaru<sup>e</sup>,  
Shigehiro Sato<sup>f</sup>, Kazuyoshi Takayama<sup>g</sup> and Hideaki Ido<sup>h</sup>

(Received November 5, 2004)

### Abstract

Energy-selective enhanced K-edge angiography utilizing a conventional x-ray generator is described. The x-ray generator is SOFRON NST-1005, and the maximum tube voltage and current are 100 kV and 5 mA, respectively. In the present research, the tube voltage ranged from 45 to 65 kV, and the tube current was regulated to optimum values. The exposure time is controlled in order to obtain optimum x-ray intensity. At a charging voltage of 60 kV, the x-ray intensity rate obtained using an aluminum and a barium sulfate filters were 58.4 and 51.6  $\mu\text{Gy/s}$  at 0.7 m per pulse, respectively, and the dimensions of the focal spot were approximately  $1 \times 1$  mm. Angiography was performed using both the aluminum and the barium sulfate filters with a charging voltage of 60 kV.

**Keywords:** angiography, aluminum filtering, barium sulfate filtering, quasi-monochromatic x rays, iodine-based contrast medium

### 1. Introduction

Monochromatic parallel radiography using a synchrotron in conjunction with single crystals continues to be the major tool used in x-ray phase imaging<sup>1,2</sup> and enhanced K-edge angiography.<sup>3,4</sup> In cases where the phase imaging is employed, the spatial resolution can be improved, and the number of tissues which can be observed using x rays increases.

To perform high-speed radiography, several different flash x-ray generators have been developed,<sup>5</sup> and soft generators<sup>6-10</sup> with photon energies of lower than 150 keV can be employed to perform biomedical

---

<sup>a</sup> Department of Physics, Iwate Medical University, 3-16-1 Honchodori, Morioka 020-0015, Japan

<sup>b</sup> Department of Nutritional Science, Faculty of Applied Bio-science, Tokyo University of Agriculture, 1-1-1 Sakuragaoka, Setagaya-ku 156-8502, Japan

<sup>c</sup> Department of Cardiac Physiology, National Cardiovascular Center Research Institute, 5-7-1 Fujishirodai, Suita, Osaka 565-8565, Japan

<sup>d</sup> Electron Tube Division #2, Hamamatsu Photonics K. K., 314-5 Shimokanzo, Toyooka Village, Iwata-gun 438-0193, Japan

<sup>e</sup> Department of Radiological Technology, School of Health Sciences, Hirosaki University, 66-1 Honcho, Hirosaki 036-8564, Japan

<sup>f</sup> Department of Microbiology, School of Medicine, Iwate Medical University, 19-1 Uchimaru, Morioka 020-8505, Japan

<sup>g</sup> Shock Wave Research Center, Institute of Fluid Science, Tohoku University, 2-1-1 Katahira, Sendai 980-8577, Japan

<sup>h</sup> Department of Applied Physics and Informatics, Faculty of Engineering, Tohoku Gakuin University, 1-13-1 Chuo, Tagajo 985-8537, Japan



radiography. In order to produce monochromatic x rays, plasma flash x-ray generators<sup>11-15</sup> are useful, since quite intense and sharp characteristic x rays such as lasers have been produced from weakly ionized linear plasmas of nickel, copper and molybdenum.

Parallel beams with photon energies of approximately 35 keV have been employed so as to perform angiography, since these beams are absorbed effectively by an iodine-based contrast medium. Subsequently, K-series characteristic x rays with energies of approximately 35 keV are also useful, and fine blood vessels were observed with high contrasts. In view of this situation, we have developed x-ray generators with cerium-target tubes<sup>16,17</sup> which can produce  $K\alpha$  rays of 34.6 keV. Because bremsstrahlung x rays of approximately 35 keV also useful in order to perform high-contrast angiography, the development of optimum filters for producing narrow-energy-latitude bremsstrahlung x rays are desired in cases where a conventional tungsten target is employed.

In this research, we employed a tungsten-target x-ray tube and performed a preliminary study on enhanced angiography achieved with bremsstrahlung x rays with narrow-photon-energy latitudes produced by filtering in conjunction with a computed radiography (CR) system.<sup>18</sup>

## 2. Principle of K-edge angiography

Figure 1 shows the mass attenuation coefficients of iodine at the selected energies; the coefficient curve is discontinuous at the iodine K-edge. The effective bremsstrahlung x-ray spectra for K-edge angiography are shown above the iodine K-edge. Because iodine contrast mediums with a K-absorption edge of 33.2 keV absorb the rays easily, blood vessels were observed with high contrasts.

## 3. Experimental setup

A steady state x-ray generator (SOFRON NST-1005) is shown in Fig. 2, and the maximum tube voltage and current are 100 kV and 5 mA, respectively. In this experiment, the tube voltage applied was from 45 to 65 kV, and the tube current was regulated to within 5.0 mA (maximum current) by the filament

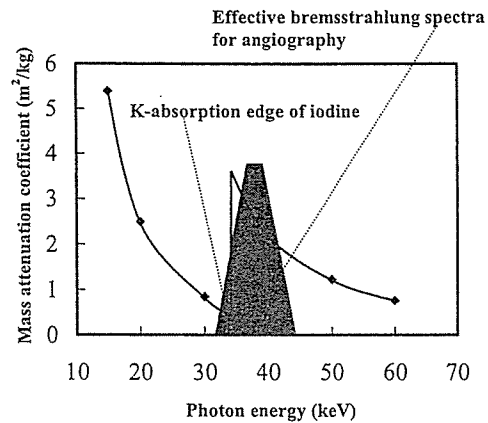


Fig. 1: Mass attenuation coefficients of iodine and effective bremsstrahlung x rays for enhanced K-edge angiography.

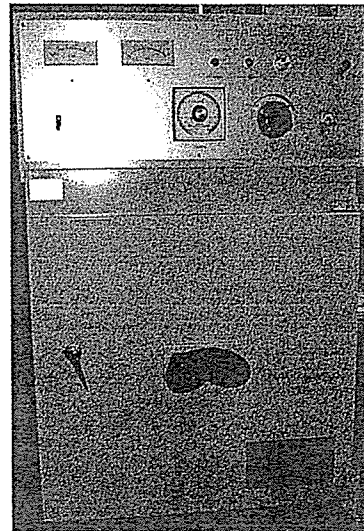


Fig. 2: X-ray generator.

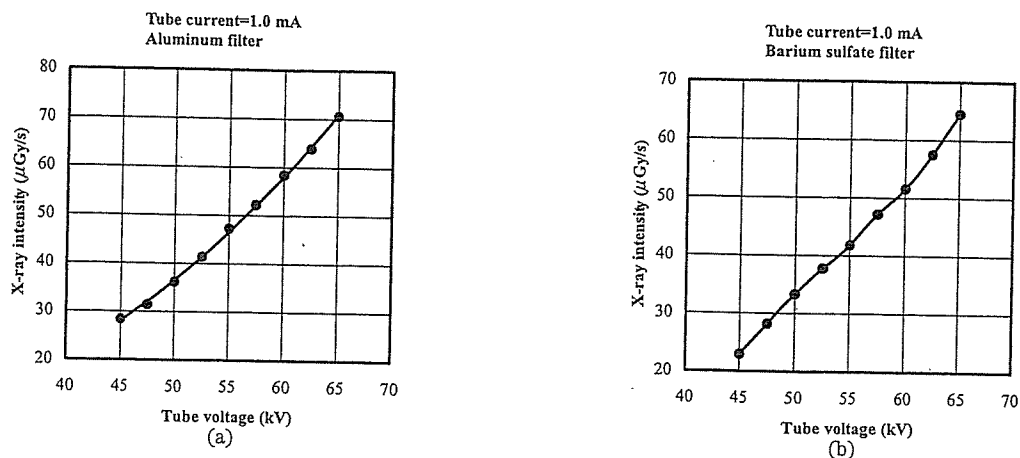


Fig. 3: X-ray intensity at 1.0 m per pulse with changing charging voltage (a) using aluminum filter and (b) using barium sulfate filter.

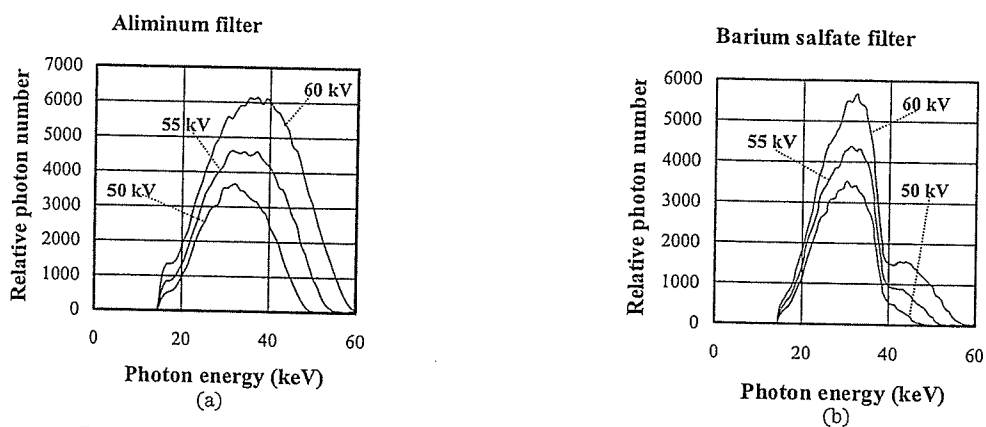


Fig. 4: X-ray spectra using (a) aluminum filter and (b) barium sulfate filter.

temperature. The exposure time is controlled in order to obtain optimum x-ray intensity. In designing the filter, the surface density of the barium sulfate powder is important, since the x rays are absorbed effectively by the powder as compared with the PMMA resin.

#### 4. Characteristics

##### 4.1 X-ray intensity

Figure 3 shows the x-ray intensity at 0.7 m per pulse measured by a Victoreen 660 ionization chamber. The x-ray intensity increased with increasing the tube voltage. At a tube voltage of 60 kV, the x-ray intensities obtained using an aluminum filter and a barium sulfate filter were 58.4 and 51.6  $\mu\text{Gy/s}$ , respectively, at 0.7 m from the x-ray source.

#### 4.2 X-ray spectra

In order to measure x-ray spectra, we employed a cadmium tellurium detector (CDTE2020X, Hamamatsu Photonics K.K.) (Fig. 4). Compared with a germanium detector, this detector has a lower energy resolution of 1.7 keV. When the tube voltage was increased, both the maximum photon energy and the intensities of bremsstrahlung x rays increased, and the photon energy of the spectrum peak also increased. The 3-mm-thick aluminum filter attenuated the low-photon-energy bremsstrahlung x rays. The barium sulfate filter, with a surface density of approximately  $10 \text{ mg/cm}^2$ , significantly attenuate the spectra above the barium K-edge energy of 37.4 keV. The areas under the spectral curves correlate closely to the total x-ray intensities shown in Fig. 3

#### 5. Angiography

The angiography was performed by the CR system (Konica Regius 150) using the filters with a tube voltage of 60 kV, and the distance between the x-ray source and the imaging plate was 0.7 m. The image contrast hardly varied even when the filter was changed.

Figure 5 shows radiograms of tungsten wires coiled around a rod made of polymethyl methacrylate using the aluminum filter. Although the image contrast increased with increases in the wire diameter, a  $50\text{-}\mu\text{m}$ -diameter wire could be observed.

Figures 6 and 7 show angiograms of a rabbit thigh (barium sulfate filter) and a dog heart (aluminum filter), respectively. In angiography, iodine-based microspheres of  $15\ \mu\text{m}$  in diameter were used, and fine blood vessels of approximately  $100\ \mu\text{m}$  were visible.

#### 6. Discussion

Concerning the spectrum measurement, we obtained bremsstrahlung x rays with narrow energy latitudes using both the aluminum and the barium sulfate filters. When the aluminum filter was employed with a tube voltage of 60 kV, the peak photon energy of spectra was approximately 35 kV.

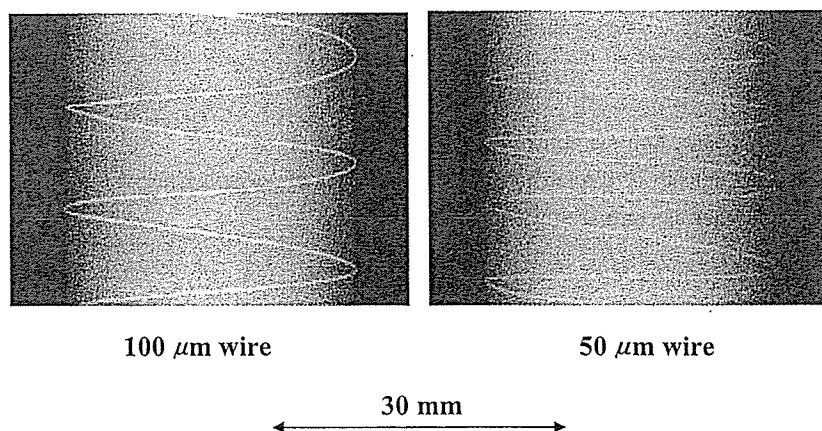


Fig. 5: Radiograms of tungsten wires coiled around rod made of polymethyl methacrylate using aluminum filter.

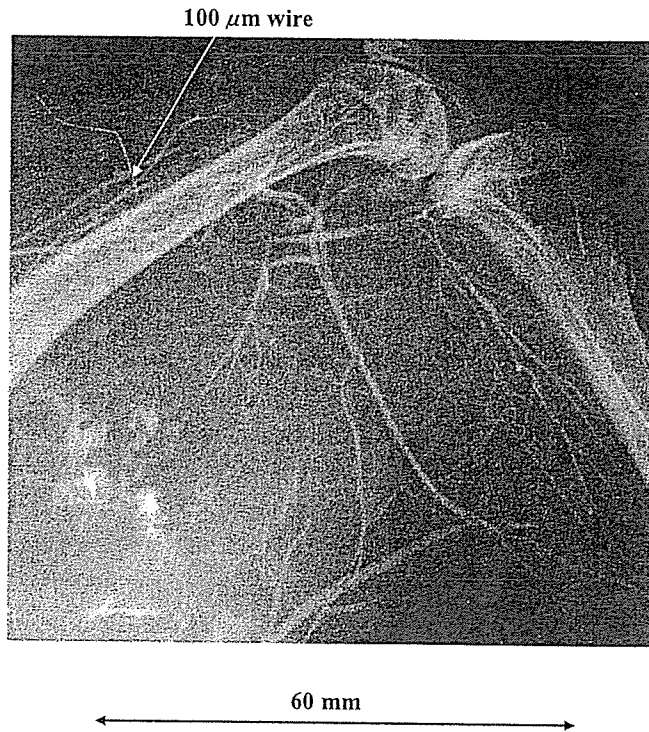


Fig. 6: Angiograms of rabbit thigh achieved with barium sulfate filter

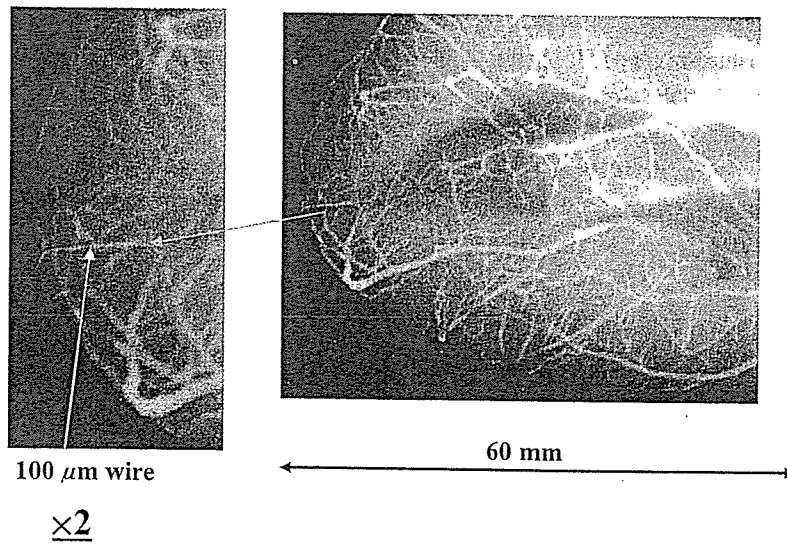


Fig. 7: Angiogram of dog heart with aluminum filter.